Proceedings of the V Brazilian Conference on Neural Networks - V Congresso Brasileiro de Redes Neurais
pp. 637–642, April 2–5, 2001 - Rio de Janeiro - RJ - Brazil

Flexible Link Control with Three Different Structures Using Feedback-Error-Learning

Areolino de Almeida Neto[1], Luiz Carlos S. Góes[2], Cairo L. Nascimento Jr. [2]
[1]Univ. Federal do Maranhão, CEP 65.085-580 São Luís-MA, Brazil
[2]Instituto Tecnológico de Aeronáutica, CEP 12228-900 São José dos Campos-SP, Brazil
E-mails: areolino@mec.ita.br, goes@mec.ita.br, cairo@ita.cta.br

Abstract

This paper discusses three structures for neural control of a flexible link using the Feedback-Error-Learning technique. This technique aims to acquire the inverse dynamic model of the plant and uses a neural network acting as an adaptive controller to improve the performance of a conventional non-adaptive feedback controller. The non-collocated control of a flexible link is characterized as a non-minimum phase system, which is difficult to be controlled by most control techniques. Three different neural approaches are used in this paper to overcome this difficulty. The first and second structures use a virtual redefined output as one of the inputs for the neural network and feedback controllers, while the third employs a delayed reference input signal in the feedback path and a tapped-delay line to process the reference input before presenting it to the neural network.

1. Introduction

There are many interests in flexible link systems, principally in some fields, for instance the aerospace industry, mainly due to the use of light-weight materials in large space structures and flexible space robots. The use of lightweight structures results in an overall system with a lower energy consumption, faster operation and lower cost. However, the control of flexible systems are more difficult to implement than the control of rigid bodies because the greater influence of unmodelled dynamics, coupling effects, structural non-linearities, and errors in the estimation of physical parameters.

In this paper, we discuss three structures that use neural network (NN) techniques to control a flexible link system. The usage of first and second approaches were proposed by [8] and the usage of third approach was proposed by [6]. All structures use a NN in a control strategy known as Feedback-Error-Learning, FEL [3] [1]. This strategy utilizes a conventional feedback controller (CFC) concurrently with a NN adapted on-line using the output of the CFC as its error signal. The CFC should at least be able to stabilize the system under control when used without the neural network. The Feedback-Error-Learning strategy aims to acquire the inverse dynamics model of the plant under control.

One great difficulty for most control strategies when dealing with flexible systems is the fact that they are in general non-minimum phase plants. In the first and second approaches this problem is surpassed by feed-backing a redefined output of the flexible system, which is also used to generate the input signal for the NN controller. In the third approach the non-minimum phase characteristic of the plant is dealt by using as the input for the CFC the comparison between a delayed reference input signal and the actual output of the flexible system while the NN controller receives the reference signal after it has been fed through a tapped-delay line [4].

This paper is structured as follows: in the second section the nonlinear mathematical model of the flexible link system is introduced and the experimental setup is presented in the third section. In the fourth section output redefinition approach for tip position control is discussed, in the fifth section the input delayed approach is investigated, in the sixth section some experimental results are presented, and in the last section conclusions are drawn.

2. Mathematical Modeling

Fig. 1 shows a structure composed of a flexible beam where one end is fixed on a rigid rotating hub and the other end is free. The flexible structure is excited by an actuator at the hub with a torque τ. The structure has a rigid body angular displacement θ and an elastic deformation $y(x,t)$, where x is the position of a point along the beam, such that $0 \le x \le l$, and l is the length of the beam. The variable to be controlled is the total angular displacement of the beam tip, v_{tip} written as $v_{tip} = \theta + y(l,t)/l$.

Considering I_h the hub inertia, r the radius of the hub, ρ the mass per unit of length of one of the flexible appendage, l the length of the appendage, m_t the mass of the accelerometer at the tip of the flexible link, the line (') and dot (.) the partial derivatives with respect to space and time, respectively, the kinetic energy of the flexible system can be expressed in the following equation:

$$T = \frac{1}{2}\rho\int_0^l (r+x)^2 dx\,\dot\theta^2 + \rho\int_0^l (r+x)\dot y dx\,\dot\theta +$$
$$\frac{1}{2}\rho\int_0^l y^2 dx + \frac{1}{2}m_t(r+l)^2\dot\theta^2 + \frac{1}{2}I_h\dot\theta^2 + \tag{1}$$
$$m_t(r+l)\dot y(l)\dot\theta + \frac{1}{2}m_t\dot y^2(l) + \frac{1}{2}m_t y^2(l)\dot\theta^2 +$$
$$I_h\dot\theta\,\dot y'(0) + \frac{1}{2}I_h\dot y'^2(0) + \frac{1}{2}\rho\int_0^l \dot y^2 dx\,\dot\theta^2$$

The elastic potential energy is:

$$V = \frac{1}{2}\int_0^l EI y''^2 dx \tag{2}$$

where E is the modulus of elasticity and I is the cross-sectional area moment of inertia. The assumed modes method is used to transform the distributed system in a discrete one. The mode shape function $\phi_j(x)$ and the characteristic equation taken are described in [5]. Applying the generalized Lagrange equation $\frac{d}{dt}\left(\frac{\partial L}{\partial \dot q}\right) - \frac{\partial L}{\partial q} = Q$, where the Lagrangian is $L = T - V$, $q = [\theta\ \eta_1\ \eta_2]^T$ (one rigid body angular displacement and two elastic modes), and $Q = [\tau\ 0\ 0]^T$, results the following matrix equation for the discrete flexible system:

$$M\ddot q + Kq + H\left[\eta\dot\theta\right] = F \tag{3}$$

where:

$$H = \begin{bmatrix} 2\dot\eta^T[MS] \\ -[MS]\dot\theta \end{bmatrix}_{(3x2)} \tag{4}$$

$$M = \begin{bmatrix} I_t + \eta^T[MS]\eta & [\mu s]_1 & [\mu s]_2 \\ [\mu s]^T{}_1 & [MS]_{11} & [MS]_{12} \\ [\mu s]^T{}_2 & [MS]_{21} & [MS]_{22} \end{bmatrix}_{(3x3)} \tag{5}$$

$$K = \begin{bmatrix} 0 & 0 & 0 \\ 0 & K_{\eta_{11}} & K_{\eta_{12}} \\ 0 & K_{\eta_{21}} & K_{\eta_{22}} \end{bmatrix}_{,(3x3)} \tag{6}$$

$$\eta = [\eta_1\,\eta_2\,]^T$$
$$[MS] = \int_0^l \rho\phi(x)\phi^T(x)dx + m_t\phi(l)\phi^T(l)$$
$$[\mu s] = \int_0^l \rho x\phi^t(x)dx + m_t l\phi^T(l) \tag{7}$$
$$[K] = \int_0^l EI\phi''(x)\phi''^T(x)dx$$
$$I_t = I_h + m_t l^2$$

$$F = [\tau\ 0\ 0]^T \tag{8}$$

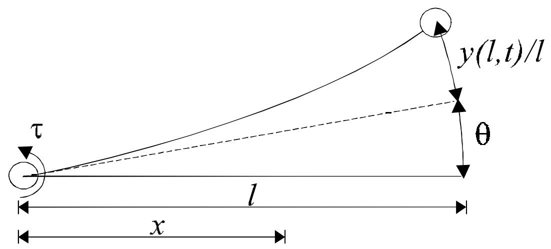

Figure 1 – Schematic of the flexible link

3. Experimental Setup

The experimental system under consideration is composed of two flexible appendages attached to a rigid hub at the middle and driven by a brushless DC motor. The output of the plant is defined by: 1) a tachometer and a potentiometer, which measure the hub angular velocity, $\dot\theta$, and the hub position, θ, respectively; 2) one accelerometer at the beam tip, which measure the tip acceleration, $\ddot y(l,t)$, and by analog integrations the tip velocity, $\dot y(l,t)$, and the tip displacement, $y(l,t)$; 3) a full strain-gage bridge which measure the elastic deformation at a known position along the beam. A cylindrical air-bearing system provides a frictionless base to the hub and the beam.

4. The Output Redefinition Approach

The output redefinition approach can be performed by two different schemes. Wang and Vidyasagar ([9]) proposed to use as output of the flexible system the so-called *reflected tip position* (RTP), v_a, defined as $v_a = h(\theta, y(l,t)) = \theta - y(l,t)/l$. Later on, Madhavan and Singh ([2]) proposed a generalized version where the output is redefined as, $v_a = \theta + \alpha\, y(l,t)/l$, where $-1 < \alpha < 1$. In this more general version, they showed that there is a critical value $0 < \alpha^* < 1$, such that for $\alpha > \alpha^*$ the zero dynamics related to this redefined output are unstable, and for $-1 < \alpha < \alpha^*$ the zero dynamics are stable. Hence, an inverse dynamics controller can be designed to control the tip position. The value of α^* depends on the payload, and it takes its smallest value when the payload is zero.

In [8] it was proposed two possible NN structures to control the tip position of the flexible link system using the redefined output v_a The first structure was called Inverse Dynamic Model Learning (IDML) and is shown in Fig. 2. The second structure was called Nonlinear Regulator Learning (NRL) and is shown in Fig. 3.

In both structures the CFC control law is $u_{cfc} = K_2(\ddot v_r - \ddot v_a) + K_1(\dot v_r - \dot v_a) + K_0(v_r - v_a)$, the learning rule for the NN is $\dot w = \gamma u_{cfc}\,\partial u_n / \partial w$, where γ

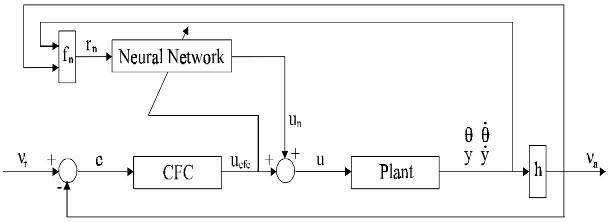

Figure 2 – Structure of the Inverse Dynamic Model Learning (IDML)

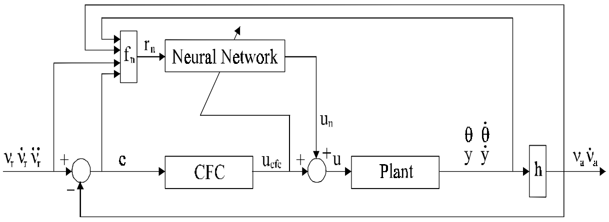

Figure 3 – Structure of the Nonlinear Regulator Learning (NRL)

is the learning rate. The NN output is $u_n = \Phi(r_n, w)$ where r_n is the NN input and w is the NN weight matrix. In the IDML structure, the NN input is calculated as $r_n = f_n(\theta, \dot\theta, y, \dot y, v_a)$, while in the NRL structure is $r_n = f_n(\ddot v_r, \dot v_r, v_r, v_r - v_a, \dot v_r - \dot v_a, \dot\theta, y, \dot y)$. In both structures the term v_r is the reference input signal for tip position and the term v_a is the redefined output. A conventional feedback controller is used as an ordinary controller to guarantee asymptotic stability during the learning period and its output is fed to the NN as its output error signal. After the learning phase, the NN should acquire an arbitrarily close model of the inverse dynamics of the plant. Then one can say that the error equation will give by $K_2\ddot e + K_1\dot e + K_0 e \cong 0$, where $e = v_r - v_a$, which means that the tracking error e should converge to zero [8].

These structures accepted any type of NN like Perceptrons, CMAC's etc. In this work we used only 3-layers Perceptrons and the training algorithm used was BackPropagation. The weights are initialized randomly between input and hidden layers and zero between hidden and output layers, in such way that at the beginning of training the output of NN is zero, so this procedure avoids to unstabilize the system at the beginning of training session. Another point used in training of NN is the learning rate used were small, in spite of large learning rate speeds up the training, this can easily unstabilize the system because can bring the NN into regions with no good minima. At all, the training goes in well-known procedure: the weights are initialized, the BP algorithm is ran and the results are obtained; if not a good result is obtained the procedure is repeated, if else then the training is stopped and the NN is considered learned.

5. The Input Delayed Approach

The structure of the adaptive control proposed by [6] is shown in the Fig. 4. The structure originally proposed by [3] is modified by the introduction of two basic modifications: a) the high-order differentiators for the reference signal were substituted by a tapped delay line of L length; and b) the input reference signal is delayed by M sampling periods ([4]) before it is compared with the **real** tip position of the beam, given by $v_{tip} = \theta + y(l,t)/l$.

Assuming that the plant is a stable SISO linear dynamic system with a transfer function $G(z)$, the linear NN transfer function is given by:

$$G^n(z) = \frac{u_n(z)}{v_r(z)} = \beta_0 + \beta_1 z^{-1} + \ldots + \beta_L z^{-L} \qquad (9)$$

Assuming that the closed loop control without the NN is stable, the polynomials $\delta(z)$ and $\psi(z)$ converge:

$$\delta(z) = \frac{G^{cfc}(z)}{1 + G(z)G^{cfc}(z)} = \sum_{j=0}^{\infty} \delta_j z^{-j} \qquad (10)$$

$$\psi(z) = \frac{G(z)G^{cfc}(z)}{1 + G(z)G^{cfc}(z)} = \sum_{j=0}^{\infty} \psi_j z^{-j} \qquad (11)$$

From the structure shown in Fig. 4, one finds:

$$u_{cfc}(z) = \left[z^{-M}\delta(z) - \psi(z)G^n(z) \right] v_r \qquad (12)$$

such that if $G_n(z) = z^{-M}/G(z)$, then $v_{tip}(z)/v_r(z) = z^{-M}$ and $u_{cfc}(z)/\ v_r(z) = 0$

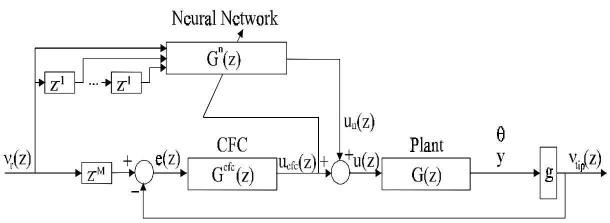

Figure 4 – Structure of input delayed approach

The NN training problem can be seen as an optimization problem, where the objective is to obtain a NN which minimizes the cost function J as defined below:

$$J = \frac{1}{2} E\left[\left(z^{-M}\delta(z) v_r(z) - \psi(z) (\beta^*)^T v_r^*(z) \right)^2 \right] \qquad (13)$$

$$\beta^* = [\beta_0 \quad \beta_1 \quad \ldots \quad \beta_L]^T \qquad (14)$$

$$v_r^*(z) = \left[v_r(z) \quad z^{-1}v_r(z) \quad \ldots \quad z^{-L}v_r(z) \right]^T \quad (15)$$

The cost function, J, will have a unique minimum if the matrix $\partial^2 J / \partial \beta^{*2}$ is positive-definite, where:

$$\partial^2 J / \partial \beta^{*2} = E\left\{ \left[\psi(z) v_r^*(z) \right] \left[\psi(z) v_r^*(z) \right]^T \right\} \underline{\Delta} F^l \quad (16)$$

The β_i parameters are found by solving the equations:

$$F^l \beta^* = F^r = E\left[\left(z^{-M} \delta(z) v_r^*(z) \right) \left(\psi(z) v_r^*(z) \right) \right] \quad (17)$$

which will have a unique solution if the input reference signal v_r has enough exciting properties, such that F^l is a positive-definite matrix. However, to calculate F^r and F^l it is necessary to know the plant transfer function $G(z)$ and its associated polynomials $\delta(z)$ and $\psi(z)$. Hence as $G(z)$ is unknown, a learning algorithm with a simple gradient descent search can be used. In this case, the following learning rule for the parameters β_i is derived:

$$\Delta\beta_i = -\gamma \left[\frac{\partial J}{\partial \beta_i} \right] = \gamma\, u_{cfc,k} \sum_{j=0}^{\infty} \psi_j v_{r,k-i-j} \quad (18)$$

Since the polynomial $\psi(z)$ is unknown, Rios Neto et al. ([7]) proposed to use another (maybe guessed) polynomial as its approximation, such that eq. 18 becomes:

$$\sigma(z) = \sum_{j=0}^{NL} \sigma_j z^{-j} \;\; \Rightarrow \Delta\beta_i = \gamma\, u_{cfc,k} \sum_{j=0}^{NL} \sigma_j v_{r,k-i-j} \quad (19)$$

6. Experimental Results

Both approaches were tested in a simulation of the system described in section 3. The input delayed approach was implemented in real time control too.

Due to the nonlinear characteristics of the flexible system as described in section 2, the linear NN was not able to converge to a good approximation of the delayed inverse dynamics. Therefore a nonlinear multilayer Perceptron was used, with input, one hidden and output layers, and trained by Back-Propagation (BP) algorithm [10]. The hidden and output network layers used hyperbolic tangent and linear functions, respectively.

The variable controlled was only the hub position. For the input delayed approach L_{input} and L_{hidden}, the number of units in the input and hidden layers, were 50 and 200, respectively, while in the IDML structure $L_{input} = 5$ and in NRL structure $L_{input} = 9$. The learning rate parameters γ_{input} and γ_{hidden} used by the BP algorithm were 0.00005 and 0.00001. The delay for the inverse model of the system in the input delayed approach (M) was 1. The simulations were performed with the minimum of variation in the parameters among the structures, in order to obtain a comparison with the same base, so the CFC gains and L_{hidden}, γ_{input} and γ_{hidden} were the same in all structures.

These parameters were adjusted empirically, except the L_{input} for IDML and NRL structures. The choice of the parameters was made considering the properties and the stability of the system, such as the time of convergence and the final performance.

A sine signal was used as the reference with a period of 6 s and amplitude equivalent to a oscillatory movement of $\pm 45^o$. During training, the period of the sine reference signal was presented 20 times. The NN took from 50 s to 80 s to converge, depending on the structure.

Fig. 5 shows the hub position curves at the end of training session for the cases simulated.

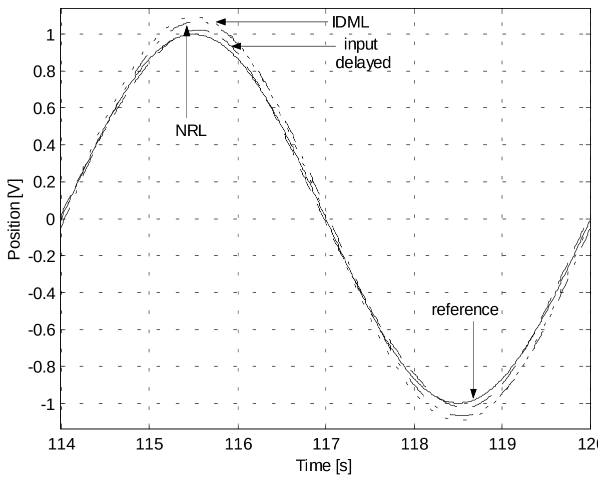

Figure 5 – Hub position curves at the end of training session

In Fig. 6 it is showed the hub position error during the training session. Fig. 7, 8 and 9 show the quadratic mean values (QMV) for the hub position error (E), the output of the CFC (Ufb), the output of the NN (Unn) and the control law ($U = Unn+Ufb$) for input delayed approach, IDML and NRL structures, respectively. In these figures, one observes that in the input delayed approach the control is more influenced by the NN at the end of training session than in the IDML and NRL structures. This evidences that in this simulation the inverse model obtained with IDML and NRL structures were not so close than obtained by the input delayed approach.

The real control implemented was only the input delayed approach. In this implementation, the sinusoidal reference with a period of 8 s and amplitude equivalent to a oscillation of $\pm 20^o$ was used. During training, a period of the sine reference signal was presented 85 times. The NN took around 200 s to converge to a good solution.

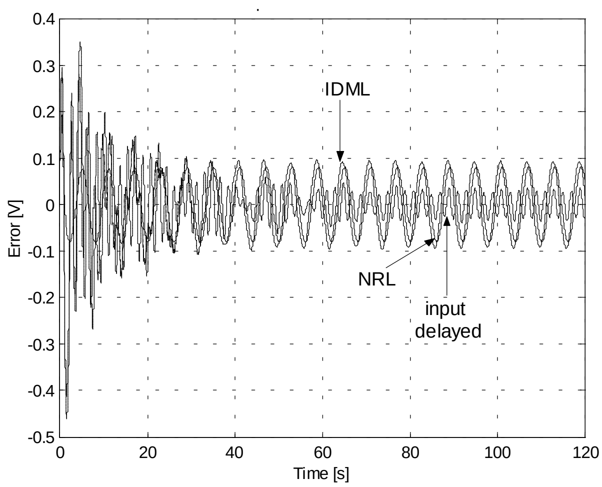

Figure 6 – Hub position error during the training session

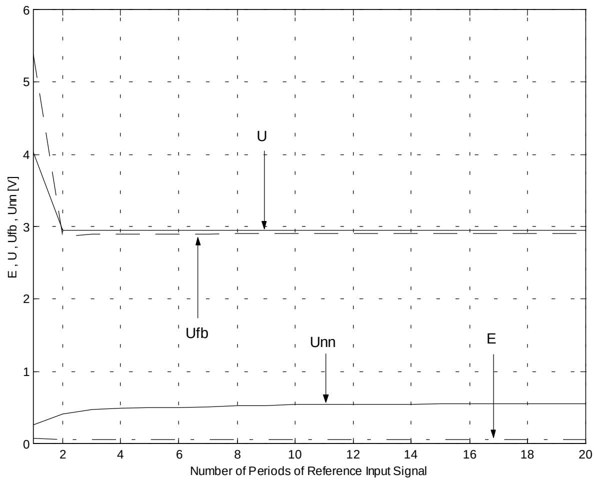

Figure 9 – Quadratic mean value obtained from NRL structure

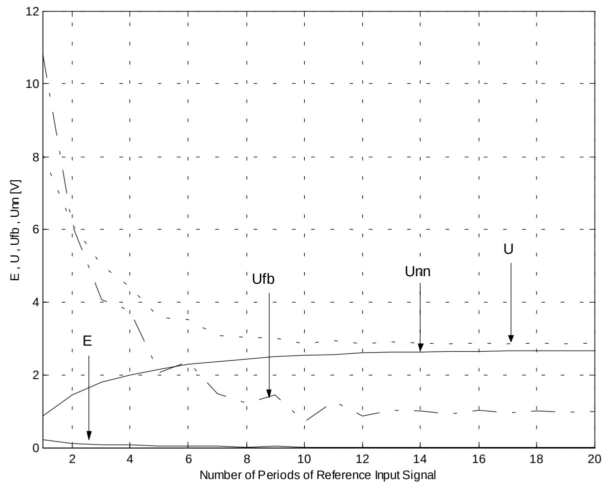

Figure 7 – Quadratic mean values obtained from input delayed approach

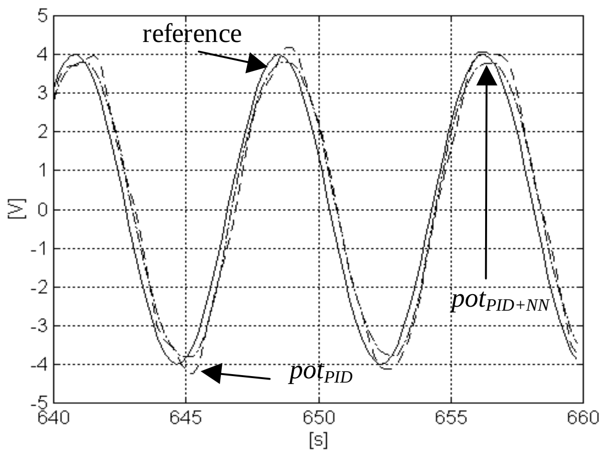

Figure 10- Comparison of the potentiometer and reference signal for the PID and PID+NN cases

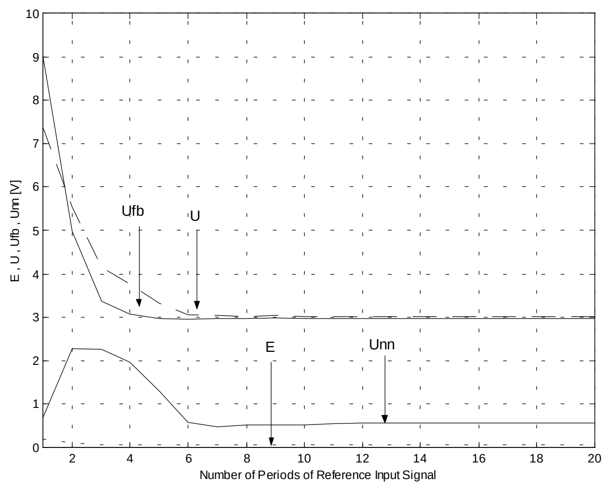

Figure 8 – Quadratic mean values obtained from IDML structure

Fig. 10 shows the input reference signal and output hub position θ at the end of the training session when the PID controller is used alone and when is used with the NN.

Fig. 11 shows the output of the tachometer for the same two cases at the end of the training session. The tachometer signal for the PID+NN case presents less harmonic content than when the PID controller was used alone, meaning that the NN was able to filter out the higher frequency mode vibration of the beam. The PID+NN controller gives an output that better resembles the sine wave reference input signal showing a better cancellation of the flexible system nonlinearities.

Fig. 12 shows the QMV of *E*, *Ufb*, *Unn* and *U* for the PID+NN case. The QMV were calculated for each period of the reference signal. This figure shows that at the end of training session, the QMV of Unn converges to the QMV of the control signal *U*, while the QMV of the CFC output and *E* are greatly reduced.

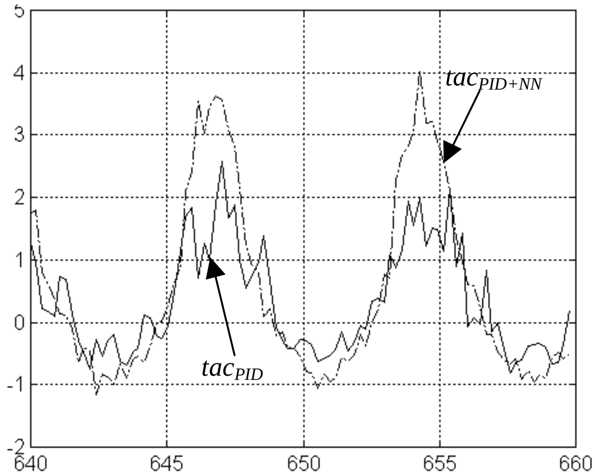

Figure 11- Comparison of the tachometer signal for the PID and PID+NN cases

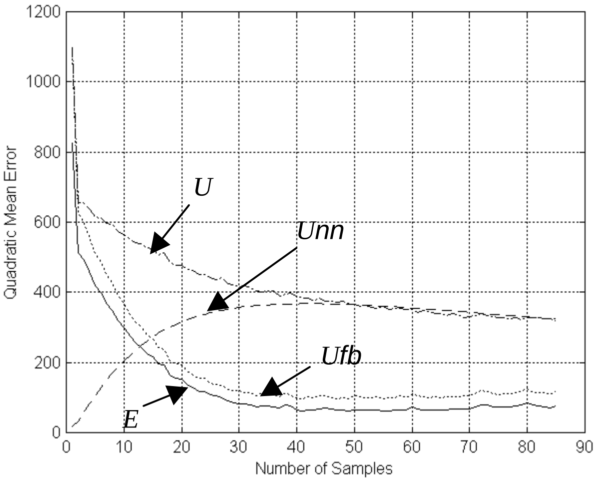

Figure 12- Quadratic mean values of *E*, *Ufb*, *Unn* and *U* for the PID+NN case

7. Conclusions

Three structures for neural control of a flexible link were presented. In simulation, the input delayed approach presented better performance, but the size of the NN was larger (weights matrix between input and hidden layer was 50x200 elements) than in IDML structure (5x200 elements) and NRL structure (9x200 elements). Further work is necessary for a better theoretical and experimental evaluation of structures controlling the same plant. In other hand, the NRL structure shows to converge faster than others, as showed by Fig. 7, 8 and 9. In these figures the QMV of *Unn* stabilize in 80 s, 50 s and 40 s, respectively. Another point to be highlighted is the control law *U* is more influenced by *Unn* in input delayed.

The experimental results obtained with the input delayed approach showed that the FEL was able to learn a good approximation of the delayed inverse dynamics of the plant, with the advantage of using the real tip position instead of a redefined virtual output of the plant as was proposed in the output redefinition approach. Effective control without excessive vibration was demonstrated by a smoother tachometer signal, as shown in Fig. 11.

References

[1] Gomi, H. and Kawato, M., "Neural Network Control for a Closed-loop System using Feedback-Error-Learning", *Neural Networks*, v. 6., pp. 933-946, 1993.

[2] Madhavan, S.K. and Singh, S.N., "Inverse Trajectory Control and Zero Dynamic Sensitivity of an Elastic Manipulator", *Int. Journal of Robotic and Automation*, pp. 179-191, 1991.

[3] Miyamoto, H., Kawato M., Setoyama T., and Suzuki, R., "Feedback Error-Learning Neural Network for Trajectory Control of a Robotic Manipulator", *Neural Networks*, I. 251-265, 1988.

[4] Nascimento Jr., Cairo L., "Artificial Neural Networks in Control and Optimization", PhD Thesis, Control Systems Centre, UMIST, UK, 1994.

[5] Rios Neto, W., "Control of a System with Flexible Appendages using Neural Networks", MSc Thesis, Technological Institute of Aeronautics, 1998 (in portuguese).

[6] Rios Neto, W., Góes, L. C., Nascimento Jr., Cairo L., "Experimental Neural Control of an Unconstrained Multibody System with Flexible Appendages", *Proceedings of the 15th Brazilian Congress of Mechanical Engineering*, 1999.

[7] Rios Neto, W., Nascimento Jr., Cairo L., Góes, L. C., "Positional Control of a Flexible Structure using Neural Networks", *Proceedings of the 4th Brazilian Conference on Neural Networks*, pp. 378-383, 1999.

[8] Talebi, H.A., Khorasani, K. and Patel, R.V., "Neural Network Based Control Schemes for Flexible Link Manipulators: Simulations and Experiments", *Neural Networks II*, pp. 1357-1377, 1998.

[9] Wang, D. and Vidyasagar, M., "Transfer Function for a Single Flexible Link", *Proceedings of the IEEE International Conference on Robotics and Automation*, pp. 1042-1047, 1989.

[10] Zurada, J. M., "*Introduction to Artificial Neural Networks*", New York, West Pub. Co., 1992.